Molecular Diversity
https://doi.org/10.1007/s11030-024-10872-2

ORIGINAL ARTICLE

An efficient methodological approach for synthesis of selenopyridines: generation, reactions, anticancer activity, EGFR inhibitory activity and molecular docking studies

Bahgat R. M. Hussein[1] · Sham M. M. El-Saghier[1] · Rasha M. Allam[2] · Mamdouh F. A. Mohamed[3] · Amer A. Amer[1]

Received: 14 January 2024 / Accepted: 9 April 2024

Abstract

In the present work, we successfully synthesized *Se*-alkyl selenopyridines **1** and **3**, selenopheno[2,3-*b*]pyridine **2**, and bis-selenopyridine **4** derivatives using an eco-friendly method by utilizing NaHSe instead of toxic hydrogen selenide. The effect of the temperature on the reaction was screening at various temperatures. The regiospecific reaction of selenopyridine **1** with bromine afforded an unexpected product 4,6-diamino-5-bromo-2-[(cyanomethyl)selenyl]-pyridine-3-carbonitrile (**5**), which was cyclized to selenopheno[2,3-*b*]pyridine (**7**) by refluxing in the presence of TEA. While its treatment with thiophenol and/or *p*-chlorothiophenol gave **8a**, **b**. On the other hand, its reaction with aminothiophenol afforded 2-(benzo[*d*]-thiazol-2-yl)-5-bromoselenopheno[2,3-*b*]pyridine-3,4,6-triamine (**9**). Also, *N*-(2-cyano-4-methyl-5*H*-1-seleno-3,5,8-triazaacenaphthylen-7-yl)acetamide (**11**) and a novel series of selenoazo dyes **12a**–**d** were synthesized by treatment of selenopheno[2,3-*b*]pyridine **2** with acetic anhydride and/or diazonium chlorides of aromatic amines, respectively. Then, we ascertained the potential activity of synthesized compounds against highly metastatic prostate cancer cells (PC-3) and osteosarcoma cells (MG-63) and found that **12a**, **12b**, **12c**, and **12d** were more cytotoxic than doxorubicin in both tested cell lines, showing nearly the same anticancer activity with IC_{50} values ranging from 2.59 ± 0.02 µM to 3.93 ± 0.23 µM. Mechanistically, the most potent compounds **12a** and **12b** proved to be potent EGFR inhibitors with IC_{50} values of 0.301 and 0.123 µM, respectively, compared to lapatinib as a positive reference ($IC_{50} = 0.049$ µM). Moreover, the docking results are in good agreement with the anticancer activity as well as the EGFR inhibitory activity, suggesting these two compounds as promising EGFR anticancer candidates.

✉ Bahgat R. M. Hussein
bahgat.ramadan@yahoo.com; bahgat@science.sohag.edu.eg

✉ Amer A. Amer
amer_chem@yahoo.com

[1] Department of Chemistry, Faculty of Science, Sohag University, Sohag 82524, Egypt

[2] Pharmacology Department, National Research Centre, Giza 11865, Egypt

[3] Department of Pharmaceutical Chemistry, Faculty of Pharmacy, Sohag University, Sohag 82524, Egypt

Published online: 13 May 2024

Graphical abstract

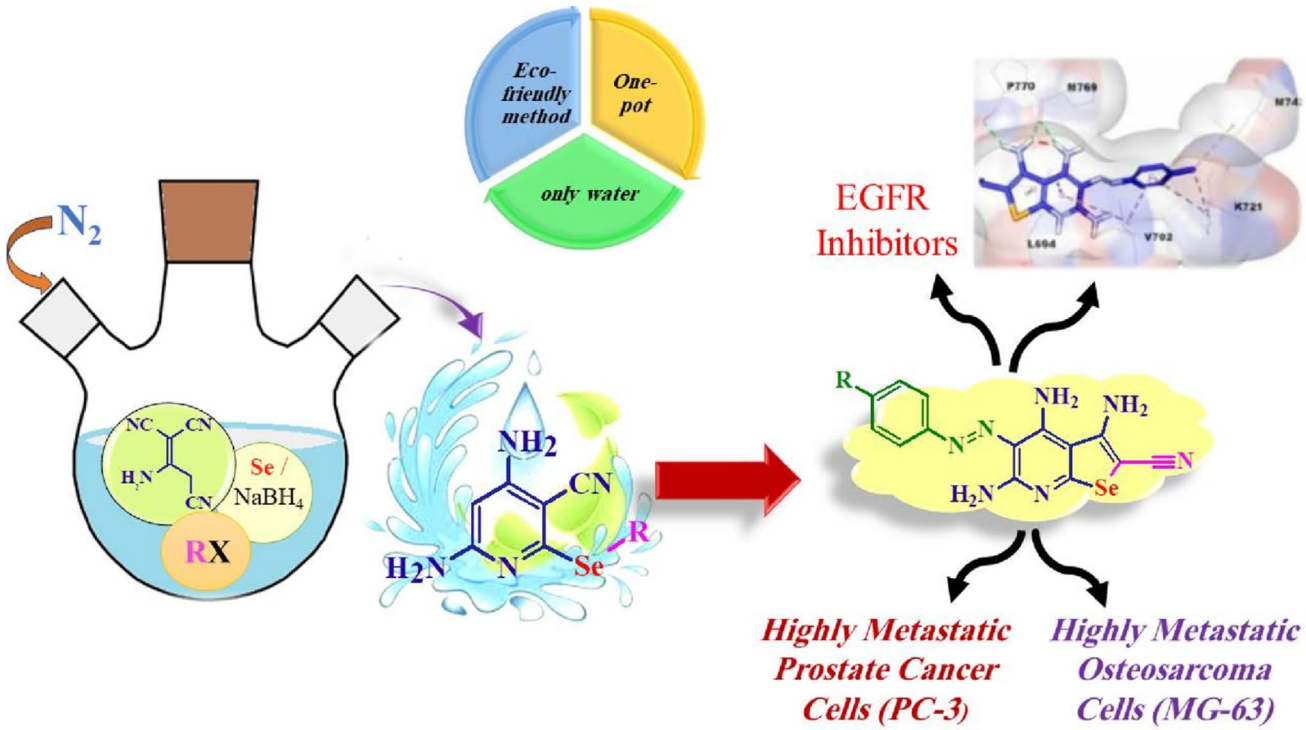

Keywords Selenopyridine · Selenopheno[2,3-*b*]pyridine · Selenoazo dyes · Anticancer · EGFR inhibitor

Introduction

Prostate cancer remains one of the most frequently diagnosed malignancies in men globally [1]. Bone metastasis is the most usual metastatic location for advanced prostate cancer, especially in the bones of the axial skeleton, such as the pelvis, spine, and ribs, where red marrow is most prevalent [2, 3]. Once bone metastasis arises, the patient survival rate drops to less than 30% [4], usually triggering several bone-related clinical manifestations such as bone pain, pathological fracture, and nerve compression syndrome that often lead to a poor prognosis for prostate cancer patients [5]. Osteosarcoma (OS) is known as the most prevalent and aggressive malignant bone disease, with a worldwide incidence of about one to three cases per million per year [6]. In addition, patients with metastatic osteosarcoma exhibit unsatisfactory responses to currently available chemotherapeutics. Therefore, discovering more effective chemotherapeutic treatments with fewer side effects is an urgent need to suppress metastasis and enhance long-term survival rates. A noteworthy concern in prostate cancer management involves identifying the factors influencing survival. Among the numerous environmental factors determining survival, particular elements have been examined, including selenium (Se) [7–9].

Selenium and Se-containing compounds have gained interest as anticancer treatments in recent decades, with numerous studies proving their great potency and selectivity against cancer cells [10, 11]. Selenium, an essential trace mineral, has been greatly researched for the development and progression of prostate cancer. These investigations have focused on its involvement in antioxidant defense [12], androgen receptor signaling [13], and cell cycle [14]. Furthermore, there is growing evidence that selenium can act as a preventive agent, and the selenium levels in the bloodstream may be correlated with the development of prostate cancer [15].

Research suggests that the epidermal growth factor receptor (EGFR), a tyrosine kinase receptor (RTK) of the ErbB family, has a substantial role in prostate cancer tumorigenesis and progression [16–18]. Previous research has linked EGFR expression to high-grade, advanced-stage prostate cancer and an increased risk of recurrence, invasion, and bone metastases [19–21]. In addition, as one of the EMT regulators, EGFR was also shown to regulate the differentiation and proliferation of osteoblasts, chondrocytes, and osteoclasts, thereby regulating cancer metastasis and

bone formation [22], and thus EGFR may be considered as a surrogate marker of prostate cancer dissemination to bones [23], supporting the rationale for the use of EGFR inhibitors for prophylaxis or cure of prostate cancer metastasis [3].

Interestingly, studies tested the anticancer activity of synthetic Se-containing compounds through their suppressive EGFR, because activation of EGFR is strongly associated with tumor growth, progression, metastasis, invasion, and poor prognosis [24, 25]. As a result, there has been a boom in research into the design and synthesis of EGFR inhibitors, sparked by accumulating evidence that they hold substantial potential in cancer treatment [26, 27]. Targeting EGFR using Se-products has shown promise in treating cancer [28, 29]. Yet, there is a shortage of comprehensive investigation to evaluate the modulatory effect of Se compounds on EGFR in prostate cancer.

Nevertheless, the synthesis of overly homogenous and stable (Se)-containing molecules remains an obstacle to their application [29]. In recent years, researchers have been more interested in organoselenium compounds and their biological effects. Selenopyridines, in particular, have received increasing attention because of their application in a variety of bioactive molecules and pharmaceuticals, such as anti-inflammatory, antioxidant activity (Fig. 1A) [30], anti-leukemic activity (Fig. 1B) [31], antimicrobial activity (Fig. 1C) [32], and antitumor activity (Fig. 1D) [33]. The anticancer characteristics of selenium and selenium-containing compounds continued to be a topic of interest in medicinal chemistry as possible scaffolds for discovering new anticancer molecules [34, 35].

Moreover, 4,6-Diamino-2-(alkylselanyl)pyridinonitriles were prepared by different methods: by passing H_2Se through an alkaline solution of malononitrile (Fig. 2a) [36], alternatively, the selenopyridines can be obtained directly by the reaction of cyanoselenoacetamide [which is obtained by passing H_2Se through a cold alkaline solution of malononitrile] with himself using EtONa as a basic catalyst [37] or by using TEA in diethyl ether [38] (Fig. 2b), as well as, selenopyridines can be obtained by the reaction of cyanoselenoacetamide with malononitrile (Fig. 2c) [38] or with 3-oxobutanamide in the basic condition (Fig. 2d) [39]. However, these methods are expensive and harmful to human health due to the use of hydrogen selenide gas, which is prepared by the reaction of selenium or selenides with acids [40] and has an unpleasant odor, is highly flammable, and is more toxic than its congener hydrogen sulfide. Furthermore, the initial effects of H_2Se on those exposed are signs of respiratory irritation, including running noses, sneezing, irritating eyes, chest tightness, and it may be irritating to bronchitis [41, 42]. Thus, from the above mention and for the continuation of our works [43–49] we aim to use an eco-friendly method in the present work for the synthesis of selenopyridines by the utilization of NaHSe instead of toxic hydrogen selenide (Fig. 2). Moreover, we studied their reactions with different reagents optimistically to synthesize novel organoselenium compounds incorporating selenopyridine moiety and assessed the sensitivity of prostate cancer and osteosarcoma cell lines to synthesized compounds compared with Doxorubicin, standard chemotherapy using an EGFR activity inhibitory assay.

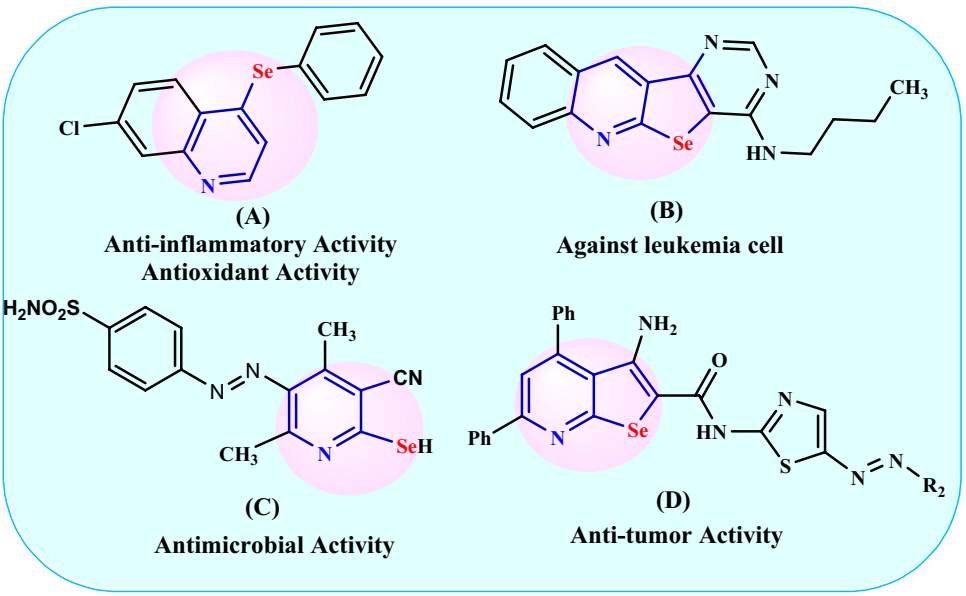

Fig. 1 Examples of biologically active selenopyridines

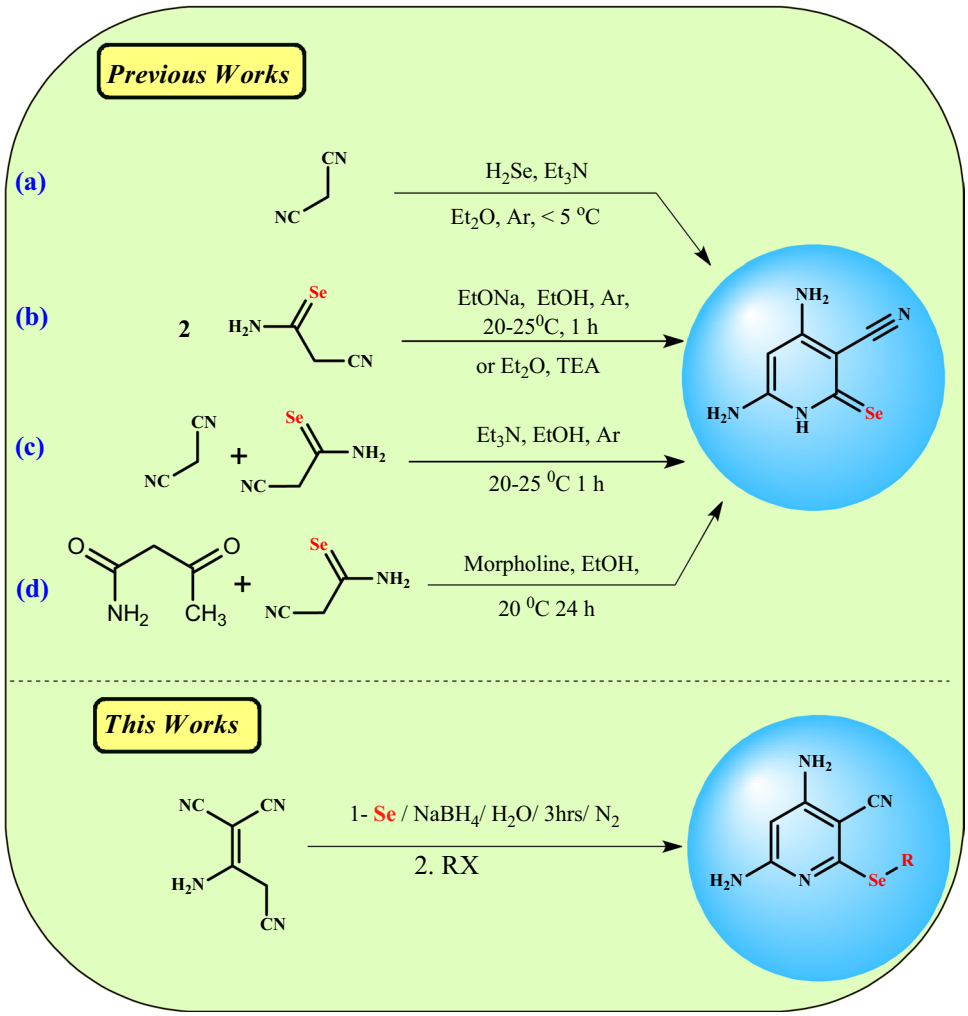

Fig. 2 Synthetic approaches to synthesizing selenopyridines using various reaction conditions

Results and discussion

Chemistry

Herein, we achieved an eco-friendly method for the synthesis of novel selenopyridines via a one-pot four-component reaction of selenium, sodium borohydride, and 2-aminoprop-1-ene-1,1,3-tricarbonitrile with an active halo-compound (Scheme 1). The initial experiment was nominated in two steps. Firstly, sodium 4,6-diamin-3-cyanopyridine-2-selenolate (intermediate **III**) was synthesized by the reaction of sodium hydrogen selenide (prepared in situ by addition of sodium borohydride to a stirred solution of selenium powder in distilled water under nitrogen in an ice bath for about 10 min) with an equivalent amount of 2-aminoprop-1-ene-1,1,3-tricarbonitrile at 80 °C for 3 h under inert conditions. Secondly, the active halo-compound, such as chloroacetonitrile was added to a stirred reaction mixture at room temperature (~30 °C with continuous stirring for 1 h. This method was mentioned by TLC to afford a mixture of selenopyridine **1** (24% yield) and selenopheno[2,3-*b*]pyridine **2** (43% yield), which are separated by column chromatography ($CHCl_3$:EtOH 10:1) (Table 1, entry 1).

Accordingly, the reaction was optimized and investigated to improve the yield and isolate compounds **1** or **2** as pure products by changing the reaction temperature. The effect of the temperature on the reaction was screening at various temperatures. The results of this screening indicated that by increasing the reaction temperature, the yield of selenopheno[2,3-*b*]pyridin **2** increased and the yield of selenopyridine **1** decreased, while the total yield generally decreased (Table 1, entries 2–4). The reaction didn't occur, and no products were separated when the reaction temperature was rising to 70 °C (Table 1, entry 5). However, decreasing the reaction temperature to 0 °C leads to the formation of 4,6-diamino-2-[(cyanomethyl) seleno]pyridine-3-carbonitrile (**1**) in a good yield (81%) without any contamination by selenopheno[2,3-*b*]pyridine **2** (Table 1, entry 6). On the other hand, 3,4,6-triamino-2-cyanoselenopheno[2,3-*b*]pyridine (**2**) was formed chemically as a pure product with an excellent yield (95%) via the

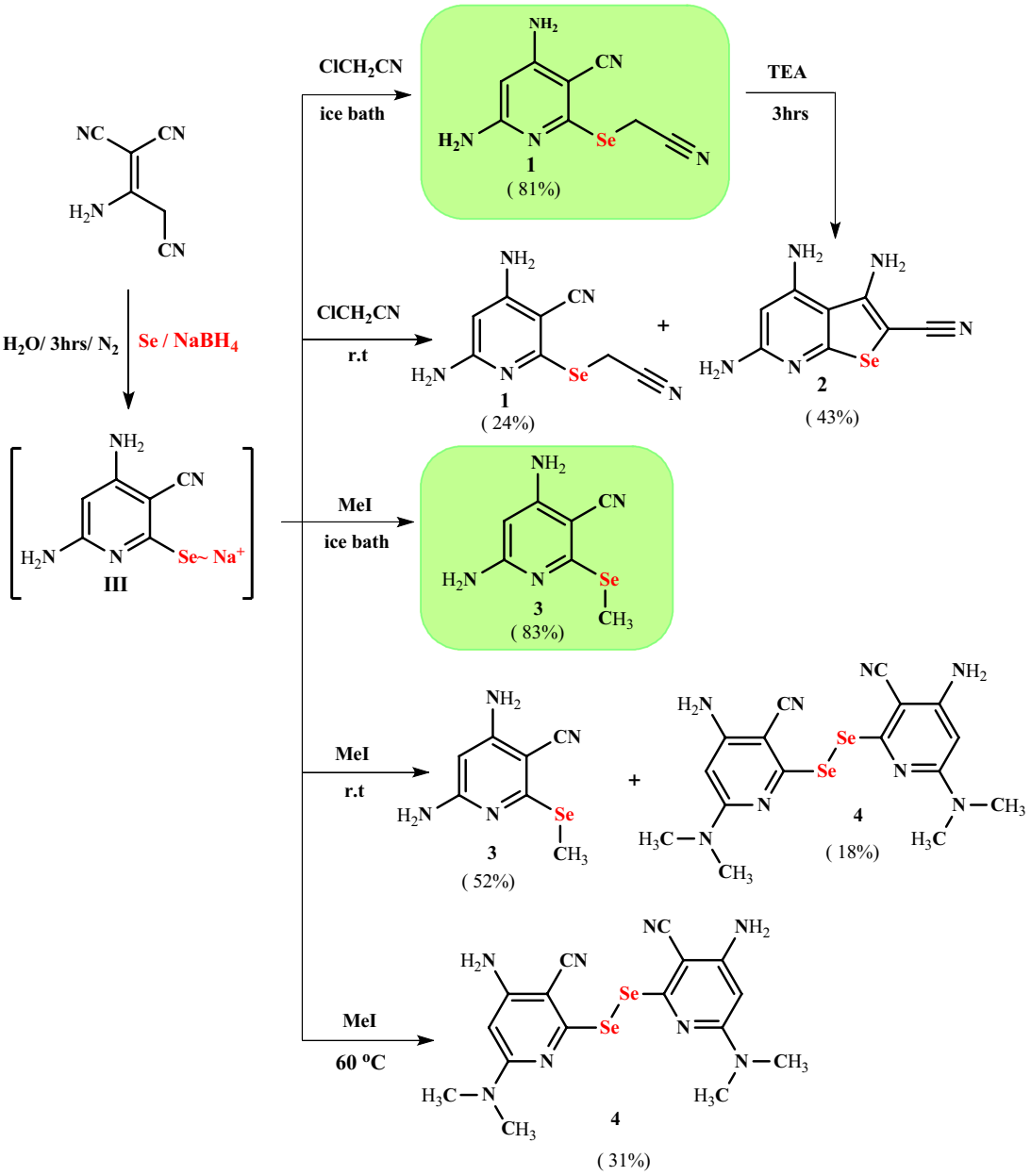

Scheme 1 Synthesis of selenopyridine **1**–**4**

refluxing of selenopyridine **1** in ethanol with a catalytic amount of TEA (Scheme 1).

On the other hand, our attempt to synthesize 4,6-diamino-2-(methylselanyl)pyridine-3-carbonitrile (**3**) via the reaction of sodium 4,6-diamino-3-cyanopyridine-2-selenolate (intermediate **III**) with methyl iodide as an active halo-compound under the same condition at room temperature gave product **3** and an unexpected product 2′-diselenobis[4-amino-6-(dimethylamino)pyridine-3-carbonitrile (**4**), in low yield (Scheme 1; Table 1, entry 7). Also, methylselanylpyridine **3** (yield 19–52%) and diselenobispyridine **4** (yield 18–31%) were separated when the reaction temperature was raised from room temperature to 50 °C, which was separated by column chromatography (silica gel, eluent $CHCl_3$:ethanol 10:1) (Table 1, entry 8, 9). A pure diselenobis[4-amino-6-(dimethylamino)pyridine-3-carbonitrile (**4**) was separated when the reaction temperature rose up to 60 °C (Table 1, entry 10, 11), while a pure methylselanylpyridine **3** was obtained in a good yield (83%) when the reaction occurred at 0 °C (Table 1, entry 12).

The chemical structures of the newly synthesized compounds **1**–**4** were assured by their spectral (IR, ^{1}H NMR, ^{13}C NMR, Dept-135) and elemental analyses (**Experimental, SI**). For example, the IR spectrum of

Table 1 Study the effect of reaction temperature on the products percentage

Entry	RX	Temp. [°C]	Product 1 (%)	Product 2 (%)	Product 3 (%)	Product 4 (%)
1	$ClCH_2CN$	30	24[a]	43[a]	–	–
2	$ClCH_2CN$	40	11[a]	23[a]	–	–
3	$ClCH_2CN$	50	7	13[a]	–	–
4	$ClCH_2CN$	60	5[a]	10[a]	–	–
5	$ClCH_2CN$	70	–[b]	–[b]	–	–
6	$ClCH_2CN$	**Ice bath**	**81**[c]	0	–	–
7	MeI	30	–	–	52[a]	18[a]
8	MeI	40	–	–	36[a]	24[a]
9	MeI	50	–	–	19[a]	28[a]
10	MeI	60	–	–	0[d]	31[c]
11	MeI	70	–	–	0[d]	31[c]
12	MeI	**Ice bath**	–	–	**83**[c]	**0**[d]

[a]Isolated yield after separation and purification

[b]Other product was detected

[c]Suitable condition for compound **1**, **3** and **4**

[d]Not detected

product **4** exhibited absorption bands at 3339, 3245 cm^{-1} due to pair equivalent NH_2, 2918 cm^{-1} due to CH aliphatic, and two equivalent nitrile groups at 2204 cm^{-1}. Its ^1H NMR spectrum showed a singlet signal corresponding to two equivalent NH_2 at 7.13 ppm, singlet signal due to an equivalent pair of $CH_{pyridyl}$ at 6.21 ppm, and two singlet signals at 2.42, 2.39 ppm for pair equivalent $N(CH_3)_2$ groups. Its ^{13}C NMR exhibited four signals at 117.6, 95.2, 6.4, and 6.3 ppm due to the equivalent pair of all nitriles, $CH_{pyridyl}$ and two $N(CH_3)_2$ groups, respectively. While aromatic carbons are characterized by four signals at 160.3, 159.9, 149.1 and 101.9 ppm, in addition to the XRD analysis showing the presence of selenium in the product **4**.

The suggested reaction mechanism for the formation of selenopyridines **3** and **4** as shown in Scheme 2 was assumed to proceed via the reaction of 2-aminoprop-1-ene-1,1,3-tricarbonitrile (**1**) with sodium hydrogenselenide (2:1 molar ratio of borohydride to selenium in water) via nucleophilic attack of the HSe^- at cyano group to form sodium salt intermediate **I**. The new imino group of intermediate **I** undergoes intramolecular cyclization via the Michael addition reaction to give intermediate **II**, which rearranges to give intermediate **III**. The intermediate **III** is less stable, so it must be reacted directly with an active halo-compound (methyl iodide) at a low temperature (in an ice bath) to give *Se*-alkyl derivative **3**. If the temperature rises more than 0 °C, the intermediate **III** rapidly oxidized to give bis-selenopyridine intermediate **IV**, which reacted with methyl iodide to give *N*-alkyl derivative **4**.

Also, the nucleophilic substitution reaction of selenopyridine **1** was studied via its reaction with bromine at room temperature in acetic acid to give the unexpected 4,6-diamino-5-bromo-2-[(cyanomethyl)selenyl] pyridine-3-carbonitrile (**5**) rather than 4,6-diamino-2-{[bromo(cyano)methyl]selenyl}pyridine-3-carbonitrile (**6**) (Scheme 3). The IR spectrum of bromoselenopyridine **5** showed the absence of CH aromatic and the appearance of the absorption bands corresponding to two NH_2 at 3470, 3412, 3344, and 3232 cm^{-1}; CH aliphatic at 2982 cm^{-1}; two nitrile groups at 2240, 2198 cm^{-1} and C=N at 1644 cm^{-1}. Moreover, its ^1H NMR spectrum showed two singlet signals corresponding to $2NH_2$ groups at 6.92, 6.64 ppm, one singlet signal due to $Se\mathbf{CH_2}$ at 4.08 ppm, while the signal attributed to $CH_{pyridyl}$ disappeared. Its ^{13}C NMR spectrum showed two signals corresponding to two CN groups at 119.6, 116.3 ppm, one singlet signal corresponding to $SeCH_2$ at 6.8 ppm, beside sp^2 carbons are characterized by five signals at 157.9, 154.8, 153.6, 83.3, and 82.6 ppm.

Bromoselenopyridine **5** was used as the starting material for the synthesis of novel products, so intermolecular cyclization of **5** was carried out by refluxing it with a catalytic amount of TEA in ethanol to afford 3,4,6-triamino-5-bromoselenopheno[2,3-*b*]-pyridine-2-carbonitrile (**7**). Also, its treatment with mono-nucleophilic reagents, namely thiophenol and *p*-chlorothiophenol, in the presence of catalytic amounts of TEA afforded the unexpected 2,2′-diselanediylbis(4,6-diamino-5-(phenylthio) pyridine-3-carbonitrile) (**8a**) and 2,2′-diselanediylbis(4,6-diamino-5-(4-chlorophenylthio)pyridine-3-carbonitrile) (**8b**), respectively (Scheme 3). On the other hand, upon reacting compound **6** with aminothiophenol under the same reaction condition, 2-(benzo[*d*]thiazol-2-yl)-5-bromoselenopheno[2,3-*b*]pyridine-3,4,6-triamine (**9**) was afforded. While its reaction with *o*-phenylenediamine and/or *o*-aminophenol gave the same unexpected product

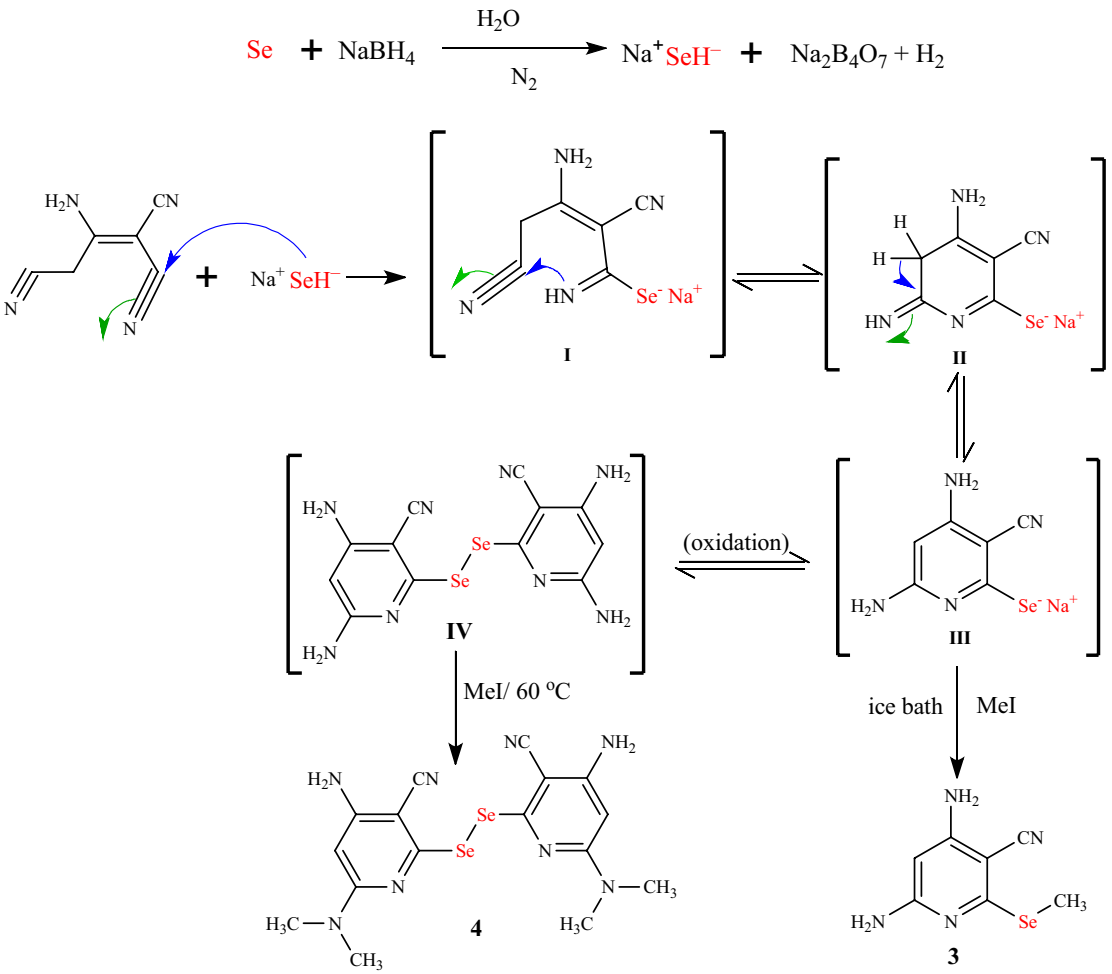

Scheme 2 Suggestion reaction mechanism for the synthesis of selenopyridines **3** and **4**

7 instead of bromoselenopheno[2,3-*b*]pyridine **10a** or **10b** (Scheme 3).

Our attempts to obtain compound **9** through the reaction of 3,4,6-triamino-5-bromoselenopheno[2,3-*b*]pyridine-2-carbonitrile (**7**) with aminothiophenol in boiling DMF in the presence of TEA as the basic catalyst failed (Scheme 3).

The IR spectrum of product **7** showed the absence of the absorption band corresponding to one C≡N group. Its ^{1}H NMR spectrum showed the absence of the absorption signal corresponding to aliphatic CH_2, while exhibiting characteristic three singlet signals corresponding to $3NH_2$ at 6.51, 6.36, and 6.15 ppm. Its ^{13}C NMR spectrum showed the disappearance of two signals for one of the cyano group and aliphatic CH_2 carbons, in addition to the increase of aromatic carbon signals at 163.7, 156.9, 154.5, 149.9, 108.0, 86.3, and 67.2 ppm, besides one signal attributed to the cyano group at 118.2 ppm. Furthermore, the IR spectrum of product **8b** showed absorption bands corresponding to pair equivalent NH_2 groups at 3453, 3337, and 3302 cm^{-1}; CH aromatic at 3085 cm^{-1}, two equivalent C≡N groups at 2236 cm^{-1} and C=N at 1617 cm^{-1}. Its ^{1}H NMR spectrum showed the aromatic protons appeared as doublet of doublet signals at 7.52–7.45 ppm with coupling constant 19 and 8 Hz, besides two singlet signals corresponding to equivalent two NH_2 groups at 6.59, 6.46 ppm (disappeared by D_2O). Its ^{13}C NMR spectrum showed the disappearance of signals corresponding to methylene and one of the nitrile groups, while it showed signals corresponding to equivalent two CN groups at 115.9 and nine signals for aromatic sp^2 carbons at 159.1, 157.8, 153.7, 135.7, 133.9, 129.6, 129.4, 82.9, and 82.8 ppm. Its Dept-135 NMR spectrum shows the disappearance of the nitrile and quaternary carbon signals and exhibited two signals corresponding to phenyl carbons (two pair equivalent 2CH) at 135.7, 129.6 ppm, in addition to the XRD analysis showing the presence of selenium in the product **8b**.

Likewise, the IR spectrum of product **9** showed the disappearance of the absorption band corresponding to two C≡N groups. Its ^{1}H NMR spectrum showed the evanescence of absorption signal corresponding to aliphatic CH_2, while

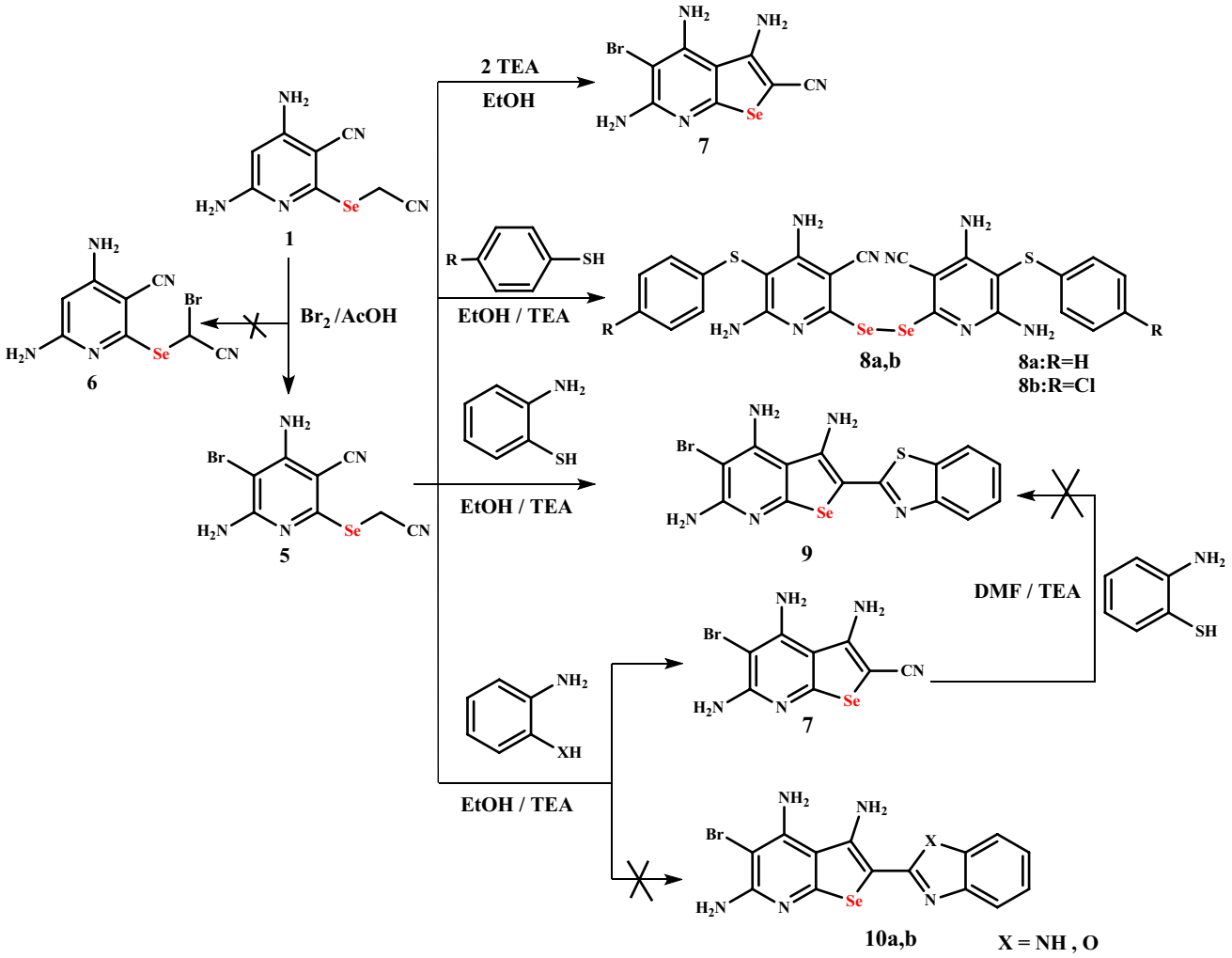

Scheme 3 Synthesis of selenopyridine **5** and selenopheno[2,3-*b*]pyridine derivatives **7–9**

it exhibited three singlet signals corresponding to three NH_2 at 6.50, 6.45, and 5.28 ppm. Whereas aromatic protons appeared as two doublet signals at 7.26 and 6.77 ppm with a coupling constant 8 Hz, in addition to two triplet signals at 7.15, 6.57 ppm with a coupling constant 7 Hz. Its ^{13}C NMR spectrum showed the disappearance of three signals for two cyano groups and sp^3 carbon of the methylene group, besides, an increase of aromatic carbon signals at 160.3, 157.6, 153.6, 151.2, 137.6, 131.5, 116.9, 116.3, 115.6, 110.7, 82.4, and 82.3 ppm.

The treatment of selenopheno[2,3-*b*]pyridine **2** with acetic anhydride afforded *N*-(2-cyano-4-methyl-5*H*-1-seleno-3,5,8-triazaacenaphthylen-7-yl)acetamide (**11**). Also, selenopheno[2,3-*b*]pyridine **2** reacted with diazonium chloride salts of aromatic amines, namely aniline, *p*-toludine, *p*-methoxyaniline, and *p*-chloroaniline, to give azo dye derivatives **12a**–**d**, respectively (Scheme 4).

The IR spectrum of seleno-3,5,8-triazaacenaphthylene **11** showed the absence of two amino groups and was exhibited by a new absorption band corresponding to 2NH groups at 3249, 3162 cm^{-1}, $CH_{aliph.}$ at 2971 cm^{-1}, the cyano group at 2180 cm^{-1} and the carbonyl group at 1673 cm^{-1}. Its ^1H NMR spectrum showed two new singlet signals due to two NH groups at 11.87, 10.79 ppm (disappeared by D_2O), singlet signal at 7.62 due to CH-6, in addition to two singlet signals at 2.23 and 2.11 ppm for CH_3 of the acetyl group and CH_3 group, respectively. Its ^{13}C NMR spectrum showed a new three signals corresponding to the carbonyl, CH_3 acetyl group, and CH_3 at 170.2, 24.6, and 22.4 ppm, respectively, in addition to CN and C-6 groups at 116.7 and 92.0 ppm, and the increase of aromatic carbon signals at 160.6, 158.9, 156.1, 155.5, 151.8, 145.6, and 116.2 ppm. Whereas the IR spectrum of azo dye **12a** showed absorption bands corresponding to three NH_2 at 3399, 3369, 3309, 3212 cm^{-1}; CH aromatic at 3022 cm^{-1}; C≡N at 2211 cm^{-1} and C=N at 1628 cm^{-1}. Its ^1H NMR spectrum showed the disappearance of $CH_{pyridyl}$ and the appearance of four singlet signals corresponding

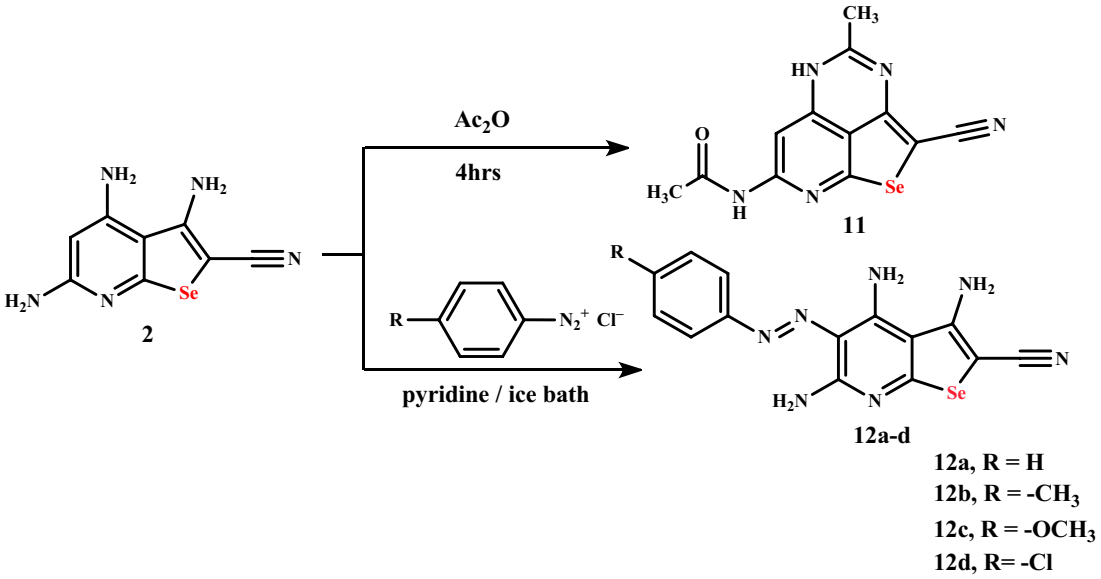

Scheme 4 Reaction of selenopheno[2,3-*b*]pyridine **2** with Ac_2O and ArN_2Cl

to three NH_2 at 11.38, 6.97, 6.38, and 5.71 ppm, beside multiple signals for the aromatic protons at 7.43–7.05 ppm and triplet signals at 7.07 ppm due to aromatic protons with a coupling constant 7 Hz. Its ^{13}C NMR spectrum showed one signal corresponding to CN groups at 115.6, while the rest of aromatic sp^2 carbons are characterized by signals at 180.1, 160.5, 160.1, 153.6, 143.2, 129.9, 123.6, 115.0, 112.5, 111.3, and 87.4 ppm.

Biology

Anticancer activity

Prostate cancer and osteosarcoma are incidental and relevant causes of death in humans. Hence, the discovery and characterization of innovative and effective medications is a current challenge [50]. While the early phases of prostate cancer are triggered by androgen production, the progression of tumor metastasis is usually androgen-independent [51]. Herein, we showed that PC-3 and MG-63 cells are not sensitive to **2**, **4**, and **7** without significant inhibition of cell proliferation (%) observed in both cell lines until 100 µM for each of them. As shown in Table 2 and Fig. 3, both compounds **9** and **11** exerted low cytotoxic effects (had high IC_{50} values ranging from in both cell lines), indicating lower potency being generally more potent in PC-3 than MG-63 cell line. Interestingly, we found that the compounds **12a**, **12b**, **12c**, and **12d** exhibited superior antiproliferative activities (i.e., they had IC_{50} values <4 µM) compared to doxorubicin (IC_{50} of 7.6 ± 0.45 µM in PC-3 and 9.4 ± 1.1 µM in MG-63) in both cell lines. Altogether, this experiment showed that compounds **12a–d** were the most potent in the panel of the investigated synthesized compounds.

Table 2 Anticancer activities of synthesized compounds against prostate cancer (PC-3) and osteosarcoma (MG-63) cell lines, IC_{50} values are expressed in µM as mean ± SD

Compounds	IC_{50} values (µM)	
	PC-3	MG-63
2	>100	>100
4	233.4 ± 2.6	239.5 ± 3.2
7	>100	>100
9	51.11 ± 3	62.84 ± 3.45
11	34.74 ± 0.77	62.17 ± 1.51
12a	2.69 ± 0.03	3.45 ± 0.2
12b	2.59 ± 0.02	3.37 ± 0.22
12c	2.75 ± 0.09	3.37 ± 0.12
12d	3.08 ± 0.01	3.93 ± 0.23
DOX	7.6 ± 0.45	9.4 ± 1.1
Lapatinib	0.13 ± 0.04	0.47 ± 0.03

Epidermal growth factor receptor activity inhibitory assay

EGFR-TK assay was carried out to investigate the EGFR inhibitory activity of the two most potent compounds **12a** and **12b**.

Interestingly, the results from the EGFR assay, as shown in Table 3, complement the findings of the cancer cell-based assay. Compound **12b** was the most potent anticancer agent and proved to be the highest EGFR inhibitor with IC_{50} values equal to 0.123 ± 0.004 µM

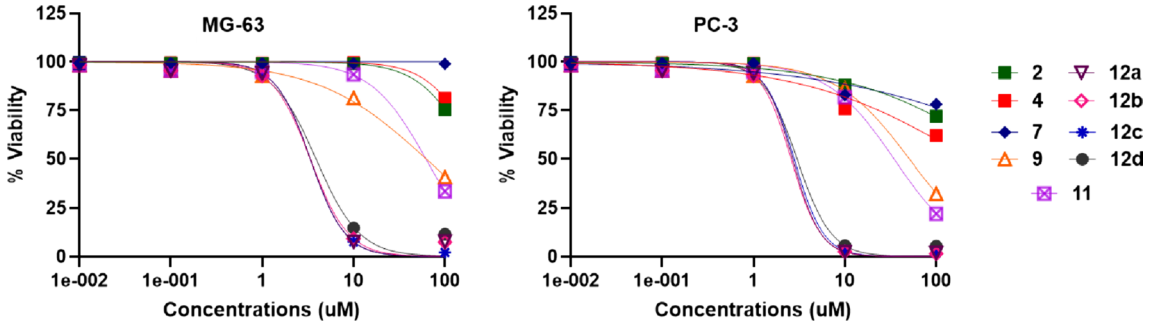

Fig. 3 The effect of synthesized compounds against the highly metastatic cancer cell lines PC-3 and MG-63 cell lines after 72 h incubation and viability was assessed by the SRB assay. Values represent the mean ± SD of three independent experiments

Table 3 Effect of compounds **12a**, **12b** and lapatinib on EGFR

Ser	Compound Code	EGFR IC_{50} (μM)
1	**12a**	0.301 ± 0.012
2	**12b**	0.123 ± 0.004
3	Lapatinib	0.049 ± 0.002

which was close to the positive reference lapatinib (IC_{50} = 0.049 μM). Compound **12a** comes next with IC_{50} value equal to 0.301 μM his assay reveals that these compounds are potent EGFR inhibitors and could possibly be used as anticancer candidates.

Docking study

The two most potent compounds **12a** and **12b** were selected for performing the docking study to achieve some structural insights into the EGFR inhibitory activities of the newly synthesized compounds using CDOCKER embedded in the Discovery Studio software (Accelrys® software corporation, San Diego, USA). The 3D crystal structure of EGFR (PDB ID: 1M17) in complex with AQ4999 was used for this docking study. As a first step, validation of the docking protocol settings was done through the re-docking of the extracted co-crystallized ligand AQ4999 from the 3D structure 1M17 using the same protocol for the docked compounds. The used docking protocol closely reproduced the bound structure with the RMSD value of 0.95 Å confirming the confidence in our docking study. Interestingly, the docking studies were consistent with the results of the EGFR inhibitory assay. The examination of docking results displayed that the two docked compounds **12a** and **12b** adopted a nearly similar disposition inside the ATP binding pocket of the EGFR. As illustrated in Fig. 4, the results of the docking study of compound **12a** (with CDOCKER interaction energy = 33.715) exhibited good fitting into the binding site of the EGFR enzyme pocket with the formation of two hydrogen bonds with Asp831 amino acids. Moreover, compound **12a** had many hydrophobic interactions such as attractive charge, pi–cation, pi–sigma, pi–sulfur, alkyl, and pi–alkyl with Asp831, Lys721, Leu820, Met742, and Cys773 amino acid residues (Fig. 4).

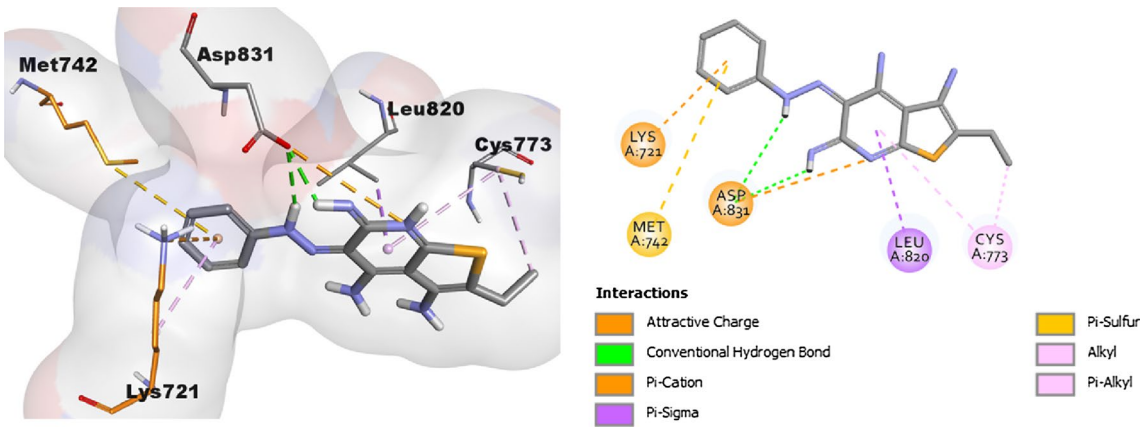

Fig. 4 2/3D Binding modes/interactions of compound **12a** into the active site of EGFR kinase (PDB code: 1M17)

Notably, analysis of the docking results of the most potent compound **12b** (with CDOCKER interaction energy = 34.125) displayed a nice fit into the pocket of the active site of the EGFR enzyme and engaged in the formation of three hydrogen bonds with Met769 (two hydrogen bonds) and Pro770 amino acids. Additionally, compound **12b** showed many hydrophobic interactions such as Van der Waals, pi–sigma, alkyl, and pi–alkyl with Leu694, Val702, Lys721 and Met742 amino acid residues as illustrated in Fig. 5.

Altogether, the docking results are in good agreement with the anticancer activity as well as the EGFR inhibitory activity, suggesting these two compounds as promising EGFR anticancer candidates.

Conclusion

An efficient eco-friendly method was developed for the synthesis of *Se*-alkyl selenopyridine and diselenobispyridine dervatives via a one-pot four-component reaction of selenium, sodium borohydride, 2-aminoprop-1-ene-1,1,3-tricarbonitrile and an active halo-compound through the preparation of in situ NaHSe instead of toxic hydrogen selenide. The effect of the reaction temperature was studied to prepare pure these products, which could be used as starting materials for the synthesis of novel bromoselenopyridine, selenopheno[2,3-*b*]pyridine, seleno-3,5,8-triazaacenaphthylene, and selenoazo dye derivatives. Most of the novel synthesized products have been evaluated for their in vitro anticancer activity against PC-3 and MG-63 cells. Among all, selenoazo dyes **12a–d** exhibited superior antiproliferative activities (i.e., they had IC_{50} values from 2.59 ± 0.02 µM to 3.93 ± 0.23 µM) compared to doxorubicin (IC_{50} of 7.6 ± 0.45 µM in PC-3 and 9.4 ± 1.1 µM in MG-63) in both cell lines. Also, the most potent compounds **12a** and **12b** proved to be potent EGFR inhibitors with IC_{50} values 0.301 and 0.123 µM, respectively, compared to lapatinib as a positive reference (IC_{50} = 0.049 µM). Moreover, the molecular docking studies for the two tested products (**12a** and **12b**) confirmed the anticancer activity and the EGFR inhibitory activity.

Experimental

Chemistry

General information

All information about reagents and spectral analyses were showed in Supporting Information.

General procedure for synthesis of selenopyridine derivatives 1 and 3

2-Aminoprop-1-ene-1,1,3-tricarbonitrile (1 g, 7.5 mmol) in 50 mL of ethanol was added to a solution of sodium hydrogen selenide [freshly prepared from finely divided selenium powder (0.59 g, 7.5 mmol) and sodium borohydride (0.56 g, 15 mmol) in 20 mL water] and the reaction mixture was refluxed under nitrogen conditions for 3 h., then cooled to room temperature and the active halo-compounds such as: chloroacetonitrile (0.57 g, 7.5 mmol) and/or methyl iodide (1 g, 7.5 mmol) was added dropwise with stirring in an ice bath for 1 h. After completion of the reaction (monitored by TLC, eluent $CHCl_3$:ethanol 10:1, Rf_1 = 0.37, and Rf_3 = 0.41), the formed precipitate was collected by filtration, washed several times with water, dried, and recrystallized from ethanol.

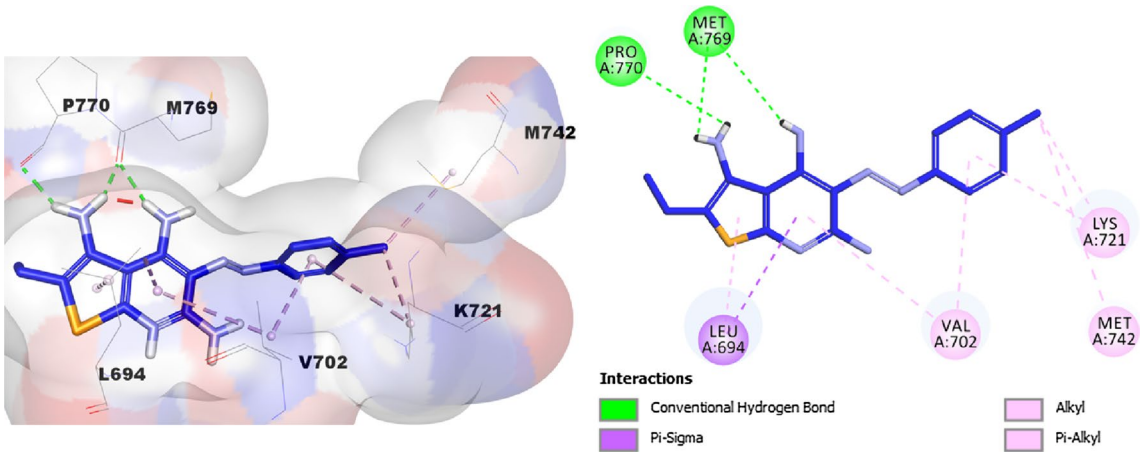

Fig. 5 2/3D Binding modes/interactions of compound **12b** into the active site of EGFR kinase (PDB code: 1M17)

4,6-Diamino-2-[(cyanomethyl)selenopyridine-3-carbonitrile (1) White crystals, yield 1.54 g (81%); mp. 160–162 °C, Lit. mp. 158–160 ℃ [38]; FT-IR (ATR) ν_{max}: 3357, 3316, 3240 ($2NH_2$), 3032 ($CH_{arom.}$), 2974 ($CH_{aliph.}$), 2234, 2190 (2C≡N), 1637 (C=N) cm^{-1}; ^1H NMR (400 MHz, DMSO-d_6): δ 6.48 (s, 2H, NH_2 exchanged by D_2O), 6.39 (s, 2H, NH_2 exchanged by D_2O), 5.53 (s, 1H, $CH_{pyridyl}$), 4.06 (s, 2H, CH_2) ppm; ^{13}C NMR (100 MHz, DMSO-d_6): δ 161.2, 157.3, 155.9, 119.8 (CN), 117.2 (CN), 85.9 ($CH_{pyridyl}$), 82.7, 6.1 (CH_2) ppm. Dept-135 NMR (100 MHz, DMSO-d_6): δ 86.1 ($CH_{pyridyl}$), 6.1 (CH_2, exchangeable) ppm. *Anal*. Calcd. For $C_8H_7N_5Se$ (252.13): C, 38.11; H, 2.80; N, 27.78% Found: C, 38.28; H, 2.93; N, 27.63%.

4,6-Diamino-2-(methylselanyl)pyridine-3-carbonitrile (3)

White crystals, yield 1.43 g (83%); mp. 148–150 °C, Lit. mp. 150–152 ℃ [38]; FT-IR (ATR) ν_{max}: 3424, 3352, 3329, 3246 ($2NH_2$), 2933 ($CH_{aliph.}$), 2203 (C≡N), 1623 (C=N) cm^{-1}; ^1H NMR (400 MHz, DMSO-d_6): δ 6.30 (s, 2H, NH_2), 6.19 (s, 2H, NH_2), 5.47 (s, 1H, $CH_{pyridyl}$), 2.35 ($SeCH_3$) ppm; ^{13}C NMR (100 MHz, DMSO-d_6): δ 161.0, 158.9, 157.1, 117.9 (CN), 85.5 ($CH_{pyridyl}$), 83.3, 5.7 ($SeCH_3$) ppm. *Anal*. Calcd. For $C_7H_8N_4Se$ (227.12): C, 37.02; H, 3.55; N, 24.67%. Found: C, 37.16; H, 3.38; N, 24.81%.

Synthesis of 3,4,6-triamino-2-cyanoselenopheno[2,3-*b*] pyridine (2)

A mixture of selenopyridine **1** (1 g, 4 mmol) and TEA (0.4 g, 4 mmol) in 20 mL of ethanol was refluxed for 3 h. After completion of the reaction (monitored using TLC, eluent $CHCl_3$:ethanol 10:1, Rf = 0.18), the excess solvent was evaporated under vacuum. The resulting product was collected and recrystallized from ethanol. Brown crystals yield 0.48 g (95%); mp. 258–260 °C, Lit mp. 256–258 ℃ [38]; FT-IR (ATR) ν_{max}: 3416, 3315, 3269, 3201 ($3NH_2$), 2164 (C≡N), 1661 (C=N) cm^{-1}; ^1H NMR (400 MHz, DMSO-d_6): δ 6.16 (s, 4H, $2NH_2$), 6.11 (s, 2H, NH_2), 5.64 (s, 1H, CH) ppm; ^{13}C NMR (100 MHz, DMSO-d_6): δ 166.0, 161.0, 155.3, 153.8, 118.9 (CN), 107.5, 88.9 (CH), 62.8 ppm. *Anal*. Calcd. For $C_8H_7N_5Se$ (252.13): C, 38.11; H, 2.80; N, 27.78%. Found: C, 37.97; H, 2.92; N, 27.81%.

Synthesis of 2,2′-diselenobis[4-amino-6-(dimethylamino) pyridine-3-carbonitrile (4)

2-Aminoprop-1-ene-1,1,3-tricarbonitrile (1 g, 7.5 mmol) in 50 mL of ethanol was added to a solution of sodium hydrogen selenide [freshly prepared from finely divided selenium powder (0.59 g, 7.5 mmol) and sodium borohydride (0.56 g, 15 mmol) in 20 mL of water] and the reaction mixture was refluxed under nitrogen conditions for 3 h, then cooled to 60 ℃, and methyl iodide (1 g, 7.5 mmol) was added dropwise with stirring for 1 h at 60 °C. After completion of the reaction (monitored by TLC, eluent $CHCl_3$:ethanol 10:1, Rf = 0.74), the formed precipitate was collected, washed with water, dried and recrystallized from ethanol. Yellow powder, yield 1.1 g (31%); mp. 172–174 °C; FT-IR (ATR) ν_{max}: 3339, 3245 (NH_2), 3043 ($CH_{arom.}$), 2918 ($CH_{aliph.}$), 2204 (C≡N), 1628 (C=N) cm^{-1}; ^1H NMR (400 MHz, DMSO-d_6): δ 7.13 (s, 4H, $2NH_2$), 6.21 (s, 2H, $2CH_{pyridyl}$), 2.42 (s, 6H, $N(CH_3)_2$), 2.39 (s, 6H, $N(CH_3)_2$) ppm; ^{13}C NMR (100 MHz, DMSO-d_6): δ 160.3, 159.9, 149.1, 117.6 (CN), 101.9, 95.2 ($CH_{pyridyl}$), 6.4 ($2NCH_3$), 6.3 ($2NCH_3$) ppm. *Anal*. Calcd. For $C_{16}H_{18}N_8Se_2$ (480.28): C, 40.01; H, 3.78; N, 23.33%. Found: C, 40.23; H, 3.62; N, 23.29%.

Synthesis of 4,6-diamino-5-bromo-2-(cyanomethylselanyl) nicotinonitrile (5)

To a solution of compound **1** (0.25 g, 2 mmol) in acetic acid (20 mL), bromine solution (0.31 g, 2 mmol) in acetic acid (5 mL) was added dropwise with stirring for about 30 min at room temperature in the presence of sunlight. After completion of the reaction (monitored by TLC, eluent $CHCl_3$:ethanol 10:1, Rf = 0.55), the formed precipitate was collected by filtration, washed by distilled water several times, dried, and recrystallized from ethanol. Brown crystal, yield 0.54 g (82%); mp. 176–178 °C; FT-IR (ATR) ν_{max}: 3470, 3412, 3344, 3232 ($2NH_2$), 2982 ($CH_{aliph.}$), 2240, 2198 (2C≡N), 1644 (C=N) cm^{-1}; ^1H NMR (400 MHz, DMSO-d_6): δ 6.92 (s, 2H, NH_2), 6.64 (s, H, NH_2), 4.08 (s, 2H, $SeCH_2$) ppm; ^{13}C NMR (100 MHz, DMSO-d_6): δ 157.9, 154.8, 153.6, 119.6 (**C**N), 116.3 (**C**N), 83.3, 82.6, 6.8 (Se**C**H_2) ppm. *Anal*. Calcd. For $C_8H_6BrN_5Se$ (331.03): C, 29.03; H, 1.83; N, 21.16%. Found: C, 29.21; H, 1.73; N, 21.32%.

Synthesis of 3,4,6-triamino-5-bromoselenopheno[2,3-*b*] pyridine-2-carbonitrile (7)

A mixture of selenopyridine **5** (1 g, 3 mmol) and TEA (0.3 g, 3 mmol) in 20 mL of ethanol was refluxed for 3 h. After completion of the reaction (monitored by TLC, silica gel, eluent $CHCl_3$:ethanol 10:1, Rf = 0.29), the formed precipitate was filtrated and recrystallized from acetone. Brown crystals, yield 0.86 g (86%); mp. 268–270 °C; FT-IR (ATR) ν_{max}: 3420, 3333, 3269 ($3NH_2$), 3051 ($CH_{arom.}$) 2177 (C≡N) cm^{-1}; ^1H NMR (400 MHz, DMSO-d_6): δ 6.51 (s, 2H, NH_2), 6.36 (s, 2H, NH_2), 6.15 (s, 2H, NH_2) ppm; ^{13}C NMR (100 MHz, DMSO-d_6): δ 163.7, 156.9, 154.5, 149.9, 118.2 (CN), 108.0, 86.3, 67.2 ppm. *Anal*. Calcd. For $C_8H_6BrN_5Se$ (331.03): C, 29.03; H, 1.83; N, 21.16%. Found: C, 29.12; H, 1.72; N, 21.21%.

General procedure for synthesis of compounds 8a,b

A mixture of compound **5** (0.5 g, 1.5 mmol), and (1.5 mmol) an appropriate thiol namely: thiophenol (0.17 g, 1.5 mmol (**Method**

A) and/or 0.34 g, 3 mmol (**Method B**) and/or *p*-chlorothiophenol (0.22 g, 1.5 mmol (**Method A**) and/or 0.44 g, 3 mmol (**Method B**) with a catalytic amount of TEA dissolved in ethanol (30 mL) and refluxed for 8 h. After completion of the reaction (monitored by TLC, eluent $CHCl_3$:ethanol 10:1, $Rf_{\mathbf{8a}} = 0.70$, $Rf_{\mathbf{8b}} = 0.74$), the excess solvent was evaporated under vacuum. The resulting product was collected and recrystallized from the appropriate solvent.

2,2'-Diselanediylbis(4,6-diamino-5-(phenylthio) pyridine-3-carbonitrile) (8a)

Brown crystal (ethanol); yield (30% Method **A**, 62% Method **B**); mp. 198–200 °C; FT-IR (ATR) ν_{max}: 3450, 3335, 3304 ($2NH_2$), 3079 ($CH_{arom.}$), 2236 (C≡N), 1617 (C=N) cm^{-1}; ^1H NMR (400 MHz, DMSO-d_6): δ 7.50–7.47 (m, 4H, $CH_{arom.}$), 7.43–7.39 (m, 6H, $CH_{arom.}$), 6.62 (s, 4H, $2NH_2$), 6.51 (s, 4H, $2NH_2$) ppm; ^{13}C NMR (100 MHz, DMSO-d_6): δ 159.5, 157.8, 153.7, 133.8, 130.6, 129.7, 128.9, 116.1 (CN), 83.3, 82.9 ppm. *Anal*. Calcd. For $C_{24}H_{18}N_8S_2Se_2$ (640.50): C, 45.00; H, 2.83; N, 17.49%. Found: C, 45.11; H, 2.91; N, 17.40%.

2,2'-Diselanediylbis(4,6-diamino-5-(4-chlorophenylthio) pyridine-3-carbonitrile) (8b)

Yellow crystal (acetone); yield (33% Method **A**, 70% Method **B**); mp. 236–238 °C; FT-IR (ATR) ν_{max}: 3453, 3337, 3302 ($2NH_2$), 3085 ($CH_{arom.}$), 2236 (C≡N), 1617 (C=N) cm^{-1}; ^1H NMR (400 MHz, DMSO-d_6): δ 7.52–7.45 (dd, 8H, $J = 19$, 8 Hz, $CH_{arom.}$), 6.59 (s, 4H, $2NH_2$ exchanged by D_2O), 6.46 (s, 4H, $2NH_2$ exchanged by D_2O) ppm; ^{13}C NMR (100 MHz, DMSO-d_6): δ 159.1, 157.8, 153.7, 135.7, 133.9, 129.6, 129.4, 115.9 (CN), 82.9, 82.8 ppm; Dept-135 NMR (100 MHz, DMSO-d_6): δ 135.7 (CH_{arom}), 129.6 (CH_{arom}) ppm. *Anal*. Calcd. For $C_{24}H_{16}C_{l2}N_8S_2Se_2$: (711.39): C, 40.63; H, 2.27; N, 15.80%. Found: C, 40.70; H, 2.19; N, 15.68%.

Synthesis of 2-(benzo[*d*]thiazol-2-yl)-5-bromo-selenopheno [2,3-*b*]-pyridine-3,4,6-triamine (9)

A mixture of compound **5** (1 g, 3 mmol) and *o*-aminothiophenol (0.377 g, 3 mmol) was refluxed in ethanol (30 mL) for 6 h in the presence of catalytic amount of TEA. After completion of the reaction (monitored by TLC, eluent $CHCl_3$:ethanol 10:1, $Rf = 0.59$), the formed precipitate was filtrated and recrystallized from acetone. Yellow crystal, yield 0.45 g (68%); mp. dec. 270–272 °C; FT-IR (ATR) ν_{max}: 3463, 3426, 3348 ($3NH_2$), 3071 ($CH_{arom.}$), 1623 (C=N) cm^{-1}; ^1H NMR (400 MHz, DMSO-d_6): δ 7.26 (d, 1H, $J = 8$ Hz, $CH_{arom.}$), 7.15 (t, 1H, $J = 7$ Hz, $CH_{arom.}$), 6.77 (d, 1H, $J = 8$ Hz, $CH_{arom.}$), 6.57 (t, 1H, $J = 7$ Hz, $CH_{arom.}$), 6.50 (s, 2H, NH_2), 6.45 (s, 2H, NH_2), 5.28 (s, 2H, NH_2) ppm; ^{13}C NMR (100 MHz, DMSO-d_6): δ 160.3, 157.6, 153.6, 151.2, 137.6, 131.5, 116.9, 116.3, 115.6, 110.7, 82.4, 82.3 ppm. *Anal*. Calcd. For $C_{14}H_{10}BrN_5SSe$ (439.19): C, 38.29; H, 2.29; N, 15.95% Found: C, 38.40; H, 2.19; N, 15.89%.

Synthesis of *N*-(2-cyano-4-methyl-5*H*-1-seleno-3,5,8-triazaacenaphthylen-7-yl)acetamide (11)

Selenopheno[2,3-*b*]pyridine **1** (0.5 g, 2 mmol) was refluxed in 15 mL of acetic anhydride for 3 h and allowed to cool at room temperature, then poured into 50 mL of cold water and left to stand for 1 h. After completion of the reaction (monitored by TLC, eluent $CHCl_3$:ethanol 10:1, $Rf = 0.25$), the formed precipitate was filtered off, washed with distilled water several times, dried, and recrystallized from ethanol. White powder, yield 0.49 g (78%); mp. ˃300 °C; FT-IR (ATR) ν_{max}: 3249, 3162, (2NH), 3013 ($CH_{arom.}$), 2971 ($CH_{aliph.}$), 2180 (C≡N), 1673 (C=O) cm^{-1}; ^1H NMR (400 MHz, DMSO-d_6): δ 11.87 (s, 1H, NH exchanged by D_2O), 10.79 (s, 1H, NH exchanged by D_2O), 7.62 (s, 1H, CH-6), 2.23 (s, 3H, CO**C**$\mathbf{H_3}$), 2.11 (s, 3H, CH_3) ppm; ^{13}C NMR (100 MHz, DMSO-d_6): δ 170.2 (C=O), 160.6, 158.9, 156.1, 155.5, 151.8, 145.6, 116.7 (CN), 116.2, 92.0, 24.6 (CO**C**$\mathbf{H_3}$), 22.4 (CH_3) ppm. *Anal*. Calcd. For $C_{12}H_9N_5OSe$ (318.19): C, 45.30; H, 2.85; N, 22.01% Found: C, 45.39; H, 2.74; N, 22.09%.

General procedure for synthesis of 3,4,6-triamino-5-[aryldiazenyl]selenopheno[2,3-*b*]pyridine-2-carbonitrile 12a–d

Sodium nitrite (0.14 g, 2 mmol) in 2 mL of cold water was added slowly at 0–5 °C to a stirred solution of appropriate aromatic amines (2 mmol) namely aniline (0.18 g), *p*-toluidine (0.21 g), *p*-methoxyaniline (0.24 g) and *p*-chloroaniline (0.25 g) in 5 mL of conc. HCl. The formed diazonium salt solution was added with continuous stirring to an ice cooled solution of selenopheno[2,3-*b*]pyridine **2** (0.5 g, 2 mmol) in 20 mL of pyridine at 0–5 °C. The reaction mixture was allowed to stand for 30 min (in an ice bath) and then poured into 50 mL cold water. After completion of the reaction (monitored by TLC, eluent $CHCl_3$:ethanol 10:1, **12a**–**d**, $Rf = 0.40, 0.48, 0.37, 0.40$, respectively), the formed precipitate filtered off, washed with distilled water several times, dried, and recrystallized from dioxane.

3,4,6-Triamino-5-[phenyldiazenyl]selenopheno[2,3-*b*] pyridine-2-carbonitrile (12a)

Beige powder, yield 0.6 g (85%); mp. dec 240–242 °C; FT-IR (ATR) ν_{max}: 3399, 3369, 3309, 3212 ($3NH_2$), 3022 ($CH_{arom.}$), 2211 (C≡N), 1628 (C=N) cm^{-1}; ^1H NMR (400 MHz, DMSO-d_6): δ 11.38 (s, 1H, NH), 7.43–7.35 (m, 4H,

$CH_{arom.}$), 7.07 (t, 1H, $J=7$ Hz, $CH_{arom.}$) 6.97 (s, 2H, NH_2), 6.38 (s, 2H, NH_2), 5.71 (s, 1H, NH) ppm.^{13}C NMR (100 MHz, DMSO-d_6): δ 180.1, 160.5, 160.1, 153.6, 143.2, 129.9, 123.6, 115.6 (CN), 115.0, 112.5, 111.3, 87.4 ppm. UV–Vis (λ_{max}, nm, DMSO): 378 nm. *Anal*. Calcd. For $C_{14}H_{11}N_7Se$ (356.24): C, 47.20; H, 3.11; N, 27.52%. Found: C, 47.36; H, 3.32; N, 27.74%.

3,4,6-Triamino-5-(4-methylphenyl)diazenylselenopheno [2,3-*b*]pyridine-2-carbonitrile (12b)

Yellow powder, yield 0.65 g (89%); mp. dec. 220–222 °C; FT-IR (ATR) ν_{max}: 3383, 3300, 3173 ($3NH_2$), 3017 ($CH_{arom.}$), 2962 ($CH_{aliph.}$), 2213 (C≡N), 1647 (C=N) cm^{-1}; ^{1}H NMR (400 MHz, DMSO-d_6): δ 11.32 (s, 1H, NH), 7.30 (d, 2H, $J=8$ Hz, $CH_{arom.}$), 7.17 (d, 2H, $J=8$ Hz, $CH_{arom.}$), 6.98 (s, 2H, NH_2), 6.35 (s, 2H, NH_2), 5.69 (s, 1H, NH), 2.27 (s, 3H, CH_3) ppm; ^{13}C NMR (100 MHz, DMSO-d_6): δ 180.1, 160.5, 160.2, 153.6, 140.9, 132.8, 130.3, 115.7 (CN), 114.4, 112.6, 111.4, 87.4, 20.8 (CH_3) ppm; UV–Vis (λ_{max}, nm, DMSO): 380 nm. *Anal*. Calcd. For $C_{15}H_{13}N_7Se$ (370.27): C, 48.66; H, 3.54; N, 26.48%. Found: C, 48.51; H, 3.73; N, 26.65%.

3,4,6-Triamino-5-[(4-methoxyphenyl)diazenyl] selenopheno[2,3-*b*]pyridine-2-carbonitrile (12c)

Reddish brown powder, yield 0.66 g (87%); mp. dec. 278–280 °C; FT-IR (ATR) ν_{max}: 3399, 3302, 3173 ($3NH_2$), 3042 ($CH_{arom.}$), 2836 ($CH_{aliph.}$), 2210 (C≡N), 1658 (C=N) cm^{-1}; ^{1}H NMR (400 MHz, DMSO-d_6): δ 11.37 (s, 1H, NH), 7.53 (s, 2H, NH_2), 7.34 (d, 2H, $J=8$ Hz, $CH_{arom.}$), 7.02 (s, 2H, NH_2), 6.96 (d, 2H, $J=8$ Hz, $CH_{arom.}$), 5.74 (s, 1H, NH), 3.75 (s, 3H, OCH_3) ppm; ^{13}C NMR (100 MHz, DMSO-d_6): δ 175.8, 159.7, 157.9, 156.3, 154.3, 136.6, 117.3 (CN), 115.2, 113.4, 112.6, 112.1, 87.1, 55.8 (OCH_3) ppm; UV–Vis (λ_{max}, nm, DMSO): 382 nm. *Anal*. Calcd. For $C_{15}H_{13}N_7OSe$ (386.27): C, 46.64; H, 3.39; N, 25.38%. Found: C, 46.72; H, 3.28; N, 25.47%.

3,4,6-Triamino-5-[(4-chlorophenyl)diazenyl] selenopheno[2,3-*b*]pyridine-2-carbonitrile (12d)

Dark yellow powder, yield 0.7 g (92%); mp. dec. 246–248 °C; FT-IR (ATR) ν_{max}: 3323, 3242, 3202 ($3NH_2$), 3060 ($CH_{arom.}$), 2215 (C≡N), 1616 (C=N) cm^{-1}; ^{1}H NMR (400 MHz, DMSO-d_6): δ 11.46 (br, 1H, NH), 7.41 (s, 4H, $CH_{arom.}$), 6.81 (s, 2H, NH_2), 6.36 (s, 2H, NH_2), 5.68 (s, 1H, NH) ppm; ^{13}C NMR (100 MHz, DMSO-d_6): δ 179.8, 160.4, 159.9, 153.5, 142.2, 129.7, 127.2, 117.2 (CN), 115.3, 112.4, 111.3, 87.5 ppm; UV–Vis (λ_{max}, nm, DMSO): 378 nm. *Anal*. Calcd. For $C_{14}H_{10}ClN_7Se$ (390.68): C, 43.04; H, 2.58; N, 25.10%. Found: C, 43.19; H, 2.42; N, 25.27%.

Biology

Anticancer activity

Cell lines and culture conditions All details about PC3 and MG-63 cells, in addition to the culture conditions were explained in Supporting Information.

Assessment of cytotoxicity by SRB assay The SRB assay was used to evaluate the effect of the synthesized selenium containing heterocyclic compounds on cancer cells according to the previous literatures [52, 53] (see Supporting Information).

EGFR inhibitory assay A cell-free assay was used to investigate the mechanism of inhibition of EGFR kinase according to the reported method [54] (see Supporting Information).

Statistical analysis All details about statistical analysis were showed in Supporting Information.

Docking study

The docking study was accomplished by using Discovery Studio software 2016 client v16.1.0.15350 (San Diego, CA) with the CDOCKER program and the 3.5 Å 3D structure of EGFR (PDB ID: 1M17) [54] in complex with AQ4999 was downloaded from the protein data bank (see Supporting Information).

Supplementary Information The online version contains supplementary material available at https://doi.org/10.1007/s11030-024-10872-2.

Author contributions All the authors BRMH, SMME, RMA, MFAM and AAA wrote the mainmanuscript text and BRMH and AAA reviewed the manuscript.

Funding Open access funding provided by The Science, Technology & Innovation Funding Authority (STDF) in cooperation with The Egyptian Knowledge Bank (EKB).

Declarations

Conflict of interest The authors declare no competing interests.

References

1. Siegel RL, Giaquinto AN, Jemal A (2024) Cancer statistics, 2024. CA Cancer J Clin 74:12–49. https://doi.org/10.3322/caac.21820
2. Wang Y, Wu N, Jiang N (2021) Autophagy provides a conceptual therapeutic framework for bone metastasis from prostate cancer. Cell Death Dis 12:909. https://doi.org/10.1038/s41419-021-04181-x
3. Wong SK, Mohamad NV, Giaze TR, Chin KY, Mohamed N, Ima-Nirwana S (2019) Prostate cancer and bone metastases: the underlying mechanisms. Int J Mol Sci 20:2587. https://doi.org/10.3390/ijms20102587
4. Foster BM, Shi L, Harris KS, Patel C, Surratt VE, Langsten KL, Kerr BA (2022) Bone marrow-derived stem cell factor regulates prostate cancer-induced shifts in pre-metastatic niche composition. Front Oncol 12:855188. https://doi.org/10.3389/fonc.2022.855188
5. Lv Z, Wang X, Zhu C, Wang K (2022) The global status of research in prostate cancer bone metastasis: a bibliometric and visualized analysis. Front Med 9:931422. https://doi.org/10.3389/fmed.2022.931422
6. Homayoonfal M, Asemi Z, Yousefi B (2022) Potential anticancer properties and mechanisms of thymoquinone in osteosarcoma and bone metastasis. Cell Mol Biol Lett 27:21. https://doi.org/10.1186/s11658-022-00320-0
7. Kenfield SA, Van Blarigan EL, DuPre N et al (2014) Selenium supplementation and prostate cancer mortality. J Natl Cancer Inst 107:dju360. https://doi.org/10.1093/jnci/dju360
8. Sayehmiri K, Azami M, Mohammadi Y et al (2018) The association between selenium and prostate cancer: a systematic review and meta-analysis. Asian Pacific J Cancer Prev 19:1431–1437. https://doi.org/10.22034/APJCP.2018.19.6.1431
9. Pietrzak S, Marciniak W, Derkacz R et al (2024) Correlation between selenium and zinc levels and survival among prostate cancer patients. Nutrients 16:527. https://doi.org/10.3390/nu16040527
10. Gandin V, Khalkar P, Braude J, Fernandes AP (2018) Organic selenium compounds as potential chemotherapeutic agents for improved cancer treatment. Free Radic Biol Med 127:80–97. https://doi.org/10.1016/j.freeradbiomed.2018.05.001
11. Radomska D, Czarnomysy R, Radomski D, Bielawski K (2021) Selenium compounds as novel potential anticancer agents. Int J Mol Sci 22:1009. https://doi.org/10.3390/ijms22031009
12. Özten N, Schlicht M, Diamond AM, Bosland MC (2014) L-Selenomethionine does not protect against testosterone plus 17β-estradiol-induced oxidative stress and preneoplastic lesions in the prostate of NBL rats. Nutr Cancer 66:825–834. https://doi.org/10.1080/01635581.2014.904907
13. Daragó A, Klimczak M, Stragierowicz J et al (2020) The effect of zinc, selenium, and their combined supplementation on androgen receptor protein expression in the prostate lobes and serum steroid hormone concentrations of Wistar rats. Nutrients 12:153. https://doi.org/10.3390/nu12010153
14. An Y, Zhao J (2021) Functionalized selenium nanotherapeutics synergizes with zoledronic acid to suppress prostate cancer cell growth through induction of mitochondria-mediated apoptosis and cell cycle S phase arrest. Front Oncol 11:1–12. https://doi.org/10.3389/fonc.2021.685784
15. Jiang J, Chen B, Tang B, Wei Q (2023) Selenium in prostate cancer: prevention, progression, and treatment. Pharmaceuticals 16:1–26. https://doi.org/10.3390/ph16091250
16. Chen T, Xu J, Fu W (2020) EGFR/FOXO3A/LXR-α axis promotes prostate cancer proliferation and metastasis and dual-targeting LXR-α/EGFR shows synthetic lethality. Front Oncol 10:1688. https://doi.org/10.3389/fonc.2020.01688
17. Liao Y, Guo Z, Xia X et al (2019) Inhibition of EGFR signaling with Spautin-1 represents a novel therapeutics for prostate cancer. J Exp Clin Cancer Res 38:1–16. https://doi.org/10.1186/s13046-019-1165-4
18. Rajput M, Singh R, Singh N, Singh RP (2021) EGFR-mediated Rad51 expression potentiates intrinsic resistance in prostate cancer via EMT and DNA repair pathways. Life Sci 286:120031. https://doi.org/10.1016/j.lfs.2021.120031
19. Day KC, Hiles GL, Kozminsky M et al (2017) HER2 and EGFR overexpression support metastatic progression of prostate cancer to bone. Cancer Res 77:74–85. https://doi.org/10.1158/0008-5472.CAN-16-1656
20. Thoma C (2017) Role for EGFR & HER2 in bone metastasis. Nat Rev Urol 14:7–7. https://doi.org/10.1038/nrurol.2016.241
21. Wang S, Wei H, Huang Z et al (2021) Epidermal growth factor receptor promotes tumor progression and contributes to gemcitabine resistance in osteosarcoma. Acta Biochim Biophys Sin (Shanghai) 53:317–324. https://doi.org/10.1093/abbs/gmaa177
22. Wells KV, Krackeler ML, Jathal MK et al (2023) Prostate cancer and bone: clinical presentation and molecular mechanisms. Endocr Relat Cancer 30:1–46. https://doi.org/10.1530/ERC-22-0360
23. Nastały P, Stoupiec S, Popęda M et al (2020) EGFR as a stable marker of prostate cancer dissemination to bones. Br J Cancer 123:1767–1774. https://doi.org/10.1038/s41416-020-01052-8
24. Makhlof MEM, Albalwe FM, Al-Shaikh TM, El-Sheekh MM (2022) Suppression effect of *Ulva lactuca* selenium nanoparticles (USeNPs) on HepG2 carcinoma cells resulting from degradation of epidermal growth factor receptor (EGFR) with an evaluation of its antiviral and antioxidant activities. Appl Sci 12:11546. https://doi.org/10.3390/app122211546
25. Han Z, He D, Zhang Y (2020) Genetic variant rs7820258 regulates the expression of indoleamine 2,3-dioxygenase 1 in brain regions. Proc Natl Acad Sci 117:24035–24036. https://doi.org/10.1073/pnas.2007022117
26. Mghwary AE-S, Gedawy EM, Kamal AM, Abuel-Maaty SM (2019) Novel thienopyrimidine derivatives as dual EGFR and VEGFR-2 inhibitors: design, synthesis, anticancer activity and effect on cell cycle profile. J Enzyme Inhib Med Chem 34:838–852. https://doi.org/10.1080/14756366.2019.1593160
27. Sun W-X, Han H-W, Yang M-K et al (2019) Design, synthesis and biological evaluation of benzoylacrylic acid shikonin ester derivatives as irreversible dual inhibitors of tubulin and EGFR. Bioorg Med Chem 27:115153. https://doi.org/10.1016/j.bmc.2019.115153
28. Crintea A, Constantin AM, Motofelea AC et al (2023) Targeted EGFR nanotherapy in non-small cell lung cancer. J Funct Biomater 14:466. https://doi.org/10.3390/jfb14090466
29. Huang J, Huang W, Zhang Z et al (2019) Highly uniform synthesis of selenium nanoparticles with EGFR targeting and tumor microenvironment-responsive ability for simultaneous diagnosis and therapy of nasopharyngeal carcinoma. ACS Appl Mater Interfaces 11:11177–11193. https://doi.org/10.1021/acsami.8b22678
30. Pinz M, Reis AS, Duarte V, da Rocha MJ, Goldani BS, Alves D, Savegnago L, Luchese C, Wilhelm EA (2016) 4-Phenylselenyl-7-chloroquinoline, a new quinoline derivative containing selenium, has potential antinociceptive and anti-inflammatory actions. Eur

J Pharmacol 780:122–128. https://doi.org/10.1016/j.ejphar.2016.03.039
31. Shahabuddin MS, Nambiar M, Choudhary B, Advirao GM, Raghavan SC (2010) A novel DNA intercalator, butylaminopyrimido[4′,5′:4,5]selenolo(2,3-b) quinoline, induces cell cycle arrest and apoptosis in leukemic cells. Invest New Drugs 28:35–48. https://doi.org/10.1007/s10637-008-9212-6
32. Abdellattif MH, Abdel-Rahman AA, Arief MM, Mouneir SM, Ali A, Hussien MA, Okasha RM, Afifi TH, Hagar M (2021) Novel 2-hydroselenonicotinonitriles and selenopheno[2,3-b] pyridines: efficient synthesis, molecular docking-DFT modeling, and antimicrobial assessment. Front Chem 9:672503. https://doi.org/10.3389/fchem.2021.672503
33. Khalifa ME, Abdel-Hafez SH, Gobouri AA, Kobeasy MI (2015) Synthesis and biological activity of novel arylazothiazole disperse dyes containing selenium for dyeing polyester fibers. Phosphorus Sulfur Silicon Relat Elem 190:461–476. https://doi.org/10.1080/10426507.2014.948622
34. Debnath S, Agarwal A, Kumar NR, Bedi A (2022) Selenium-based drug development for antioxidant and anticancer activity. Futur Pharmacol 2:595–607. https://doi.org/10.3390/futurepharmacol2040036
35. Domínguez-Álvarez E, Rácz B, Marć MA et al (2022) Selenium and tellurium in the development of novel small molecules and nanoparticles as cancer multidrug resistance reversal agents. Drug Resist Updat 63:100844. https://doi.org/10.1016/j.drup.2022.100844
36. Litvinov VP, Dyachenko VD (1999) Cyanoselenoacetamides—new convenient reagents for synthesis of functionally substituted pyridine-2-selenones, 1,4-dihydropyridine-2-selenols, and selenazoles. Russ J Org Chem 35:1377–1384
37. Nesterov VN, Shklover VE, Struchkov YuT, Sharanin YuA, Dyachenko VD (1989) Synthesis and properties of 4,6-diamino-3-cyano-2 (1*H*)-pyridineselenone: molecular and crystal structure of 2-allylseleno-4,6-diamino-3-cyanopyridine. Bull Acad Sci USSR Div Chem Sci 38:2372–2376
38. Dyachenko VD, Sharanin YuA, Litvinov VP, Nesterov VN, Shklover VE, Struchkov YuT, Promonenkov VK, Turov AV (1991) Cyclization of nitriles. XLIII. Synthesis and reactions of 4,6-diamino-3-cyano-2(1*H*)pyridineselenone. Crystal structure of 2-allylseleno-4,6-diamino-3-cyanopyridine. Zh Obshch Khim 61:747–753
39. Dyachenko VD (2005) Synthesis of ammonium 5-arylcarbamoyl-4-heteryl-6-methyl-3-cyano-1, 4-dihydropyridine-2-thiolates and 4-heteryl-5-carbamoyl-6-methyl-3-cyano-1, 4-dihydropyridine-2-selenolates. Russ J Org Chem 75:447–456
40. Fehér F (1963) Sulfur, selenium, tellurium. Handbook of preparative inorganic chemistry, 2nd edn. Academic, pp 341–456
41. Malczewska-Toth B (2012) Phosphorus, selenium, tellurium, and sulfur. Patty's toxicology. Wiley, pp 841–884. https://doi.org/10.1002/0471435139.tox044.pub2
42. Friberg L, Norberg GF, Vouk V (1986) Selenium. Handbook on the toxicology of metals, 2nd edn. Elsevier Science, Amsterdam, pp 664–679
43. Ghattas ABAG, Khodairy A, Moustafa HM, Hussein BRM (2017) New heterocyclic compounds derived from 4,6-diamino-3-cyano-2-methylthio-pyridine and their biological activity. J Heterocyclic Chem 54:879–888. https://doi.org/10.1002/jhet.2649
44. Ghattas ABAG, Khodairy A, Moustafa HM, Hussein BRM (2015) Synthesis and biological evaluation of some novel thienopyridines. J Pharm Appl Chem 1:21–26. https://doi.org/10.1278/jpac/010103
45. Ghattas ABAG, Khodairy A, Moustafa HM, Hussein BRM, Farghaly MM, Aboelez MO (2017) Synthesis, in vitro antibacterial and in vivo anti-inflammatory activity of some new pyridines. Pharm Chem J 51:652–660. https://doi.org/10.1007/s11094-017-1670-8
46. Hussein BRM, Ali AM (2019) Multicomponent reaction for synthesis of novel 2-tosyloxyphenylpyridines. J Heterocyclic Chem 56:1420–1425. https://doi.org/10.1002/jhet.3521
47. Amer AA (2018) Synthesis of some new polyfunctionalized pyridines. J Heterocyclic Chem 55:297. https://doi.org/10.1002/jhet.3049
48. Amer AA, Abdelhamid AA (2017) Microwave-assisted, one-pot multicomponent synthesis of some new cyanopyridines. J Heterocyclic Chem 54(6):3126–3132. https://doi.org/10.1002/jhet.2926
49. Abdel-Ghany H, El-Sayed AM, Amer AA, Ahmed AM (2016) Synthesis of novel fused heterocycles based on 6-amino-4-phenyl-2-thioxo-1,2-dihydropyridine-3,5-dicarbonitrile. J Heterocyclic Chem 53:2013. https://doi.org/10.1002/jhet.2522
50. Guedes JP, Pereira CS, Rodrigues LR, Côrte-Real M (2018) Bovine milk lactoferrin selectively kills highly metastatic prostate cancer PC-3 and osteosarcoma MG-63 cells in vitro. Front Oncol 8:200. https://doi.org/10.3389/fonc.2018.00200
51. Saeedi Sadr A, Ehteram H, Seyed Hosseini E, Alizadeh Zarei M, Hassani Bafrani H, Haddad Kashani H (2022) The effect of irisin on proliferation, apoptosis, and expression of metastasis markers in prostate cancer cell lines. Oncol Ther 10:377–388. https://doi.org/10.1007/s40487-022-00194-4
52. Hassabo AA, Abdelraof M, Allam RM (2023) L-Arginase from *Streptomyces diastaticus* MAM5 as a potential therapeutic agent in breast cancer: purification, characterization, G1 phase arrest and autophagy induction. Int J Biol Macromol 224:634–645. https://doi.org/10.1016/j.ijbiomac.2022.10.152
53. Le Berre M, Gerlach JQ, Dziembała I, Kilcoyne M (2022) Calculating half maximal inhibitory concentration (IC_{50}) values from glycomics microarray data using GraphPad Prism. Glycan Microarrays Methods Protoc 2460:89–111. https://doi.org/10.1007/978-1-0716-2148-6_6
54. Abou-Zied HA, Youssif BGM, Mohamed MFA, Hayallah AM, Abdel-Aziz M (2019) EGFR inhibitors and apoptotic inducers: design, synthesis, anticancer activity and docking studies of novel xanthine derivatives carrying chalcone moiety as hybrid molecules. Bioorg Chem 89:102997. https://doi.org/10.1016/j.bioorg.2019.102997